

Effects of biofilms on limestone specimens in the context of cultural heritage preservation

Davide Ripamonti¹ [0009-0008-6470-226X], Alessia Marzanni² [0009-0001-3150-3108], Chao Gao³ [0000-0003-4023-0970], Chiara Bertolin³ [0000-0002-0684-8980], Francesca Cappitelli⁴ [0000-0003-1237-1813], Villa Federica⁴ [0000-0003-1237-1813] and Nicola Gherardo Ludwig¹ [0000-0002-2589-582X]

¹ Università degli Studi di Milano, Department of Physics “A. Pontremoli”, via Celoria 16, 20133 Milano, Italy

² Libera Università di Bolzano, Faculty of Agricultural, Environmental and Food Sciences, Piazza Università 5, 39100 Bolzano, Italy

³ Norwegian University of Science and Technology, Department of Mechanical and Industrial engineering, Richard Birkelands vei 2B, Trondheim, 7491, Norway

⁴ Università degli Studi di Milano, Department of Food, Environmental and Nutritional Sciences, Via Celoria 2, 20133 Milano, Italy

Abstract. Stone surfaces are colonized by subaerial biofilms (SABs), complex multicellular communities embedded in a self-produced matrix of hydrated extracellular polymeric substances (EPS). Recent studies have shown that the SABs on artistic surfaces are not only detrimental, leading to biodeterioration, but they can also have a protective role. This is especially true for porous stones, where the SABs form a protective interface layer between the lithic material and the surrounding environment. This study reproduced mono and dual-species SABs on limestone coupons to examine stone surface properties with both living and dead SABs under moist (75% RH) and dry (30% RH) conditions. The objectives were twofold: 1) to study how live SABs impact surface water absorption and wettability in short-term experiments under different environmental conditions and 2) to explore whether dead SABs influence surface water dynamics as much as live SABs in long-term experiments.

Well-known, non-invasive analyses were employed to characterize the samples, such as microscopic observations, contact angle measurements, colorimetric and water content evaluation, and a specific Infrared thermography analysis called Spilling Drop Test. The analyses were carried out before and after exposing the biofilms to different environmental conditions, including changes in relative humidity (RH) or exposure time; the results showed that SABs modified the water sorption of materials, creating a layer at the stone-air interface. These findings open new opportunities to harness microbiological growth for protecting stone surfaces from environmental stressors. Unlike traditional conservation strategies that rely on synthetic hydrophobic coatings—which are often associated with material incompatibility, long-term degradation, and environmental concerns—SABs may act as an eco-friendly, natural barrier against moisture penetration and weathering in limestone.

Keywords: limestone, subaerial biofilm, EPS, alternative to synthetic hydro-repellant, sustainable conservation strategies.

1. Introduction

Safeguarding the historical and cultural identity embodied in stone monuments ensures that future generations can appreciate the legacy of past civilizations. However,

stone heritage (SH) is vulnerable to deterioration caused by physical, chemical, and biological processes [1, 2]. SH is colonized by subaerial biofilms (SABs) i.e. microbial ecosystems finely tuned to the atmosphere and the stone [3]. SABs rely on phototroph–chemoorganotroph partnerships and take advantage of the self-produced matrix of extracellular polymeric substances (EPSs)—mainly proteins and polysaccharides—to adhere to surfaces, conserve energy and nutrients, and coordinate survival strategies [4,5]. These features protect SAB-dwelling cells from external stresses, making them highly resistant and resilient to cleaning treatments [6]. The growth of SABs on SH has long been associated with a threat to conservation called biodeterioration [7, 8, 9]. However, recent studies show the complex interaction between SABs and the surfaces they colonize, leading to changes—often positive—in the stone’s properties, such as surface porosity and permeability [10, 11]. Thus, understanding how SABs impact lithic substrates is essential for determining whether they contribute to biodeterioration or bioprotection.

In this work, mono and dual-species SABs were grown on limestone coupons and exposed to dry (30% RH) and moist (75% RH) conditions. The objectives were twofold: 1) to study how live SABs impact surface water absorption and wettability in short-term experiments under different environmental conditions and 2) to explore whether dead SABs influence surface water dynamics as much as live SABs in long-term experiments. Since water is a key factor influencing microbial growth and stone weathering [12][13], any interference with surface water dynamics could have implications for SH conservation. This study demonstrates that SABs effectively reduce surface water absorption and diffusion while also offering biomaterials as sustainable alternatives to synthetic water-repellent coatings.

2. Materials

SAB growth on limestone. Axenic cultures of the photosynthetic cyanobacterium *Synechocystis* sp. PCC 6803 and the chemoorganotrophic bacterium *Escherichia coli* K12 MG1655 were grown in Blue-Green (BG11) and Luria-Bertani (LB) media, respectively, as per Villa et al. 2015 [14]. Stationary-phase cultures were centrifuged, rinsed with BG11, and resuspended to $\sim 10^8$ cells/ml. Equal volumes of each culture were mixed, while mono-cultures were diluted to $\sim 5 \times 10^7$ cells/ml. Mono-species (*Synechocystis* sp.) and dual-species (*Synechocystis* sp. + *E. coli*) SABs were grown in a modified Drip Flow Reactor (DFR) reported in [14].

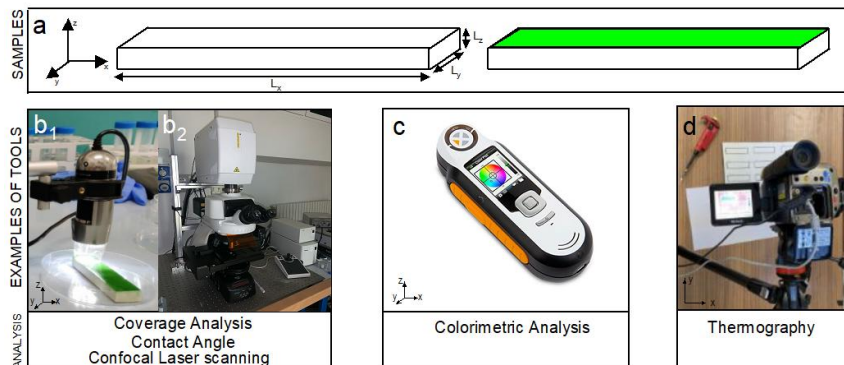


Fig 1. (a) Geometry of a control sample and example of biofilm coverage; (b) tools carried on for visible investigation and characterization, (b₁) digital microscope, (b₂) confocal Laser Scanning Microscopy; (c) colorimeter instrument; (d) infrared thermal camera.

Identical limestone specimens (Fig. 1a, L_x 75 mm \times L_y 23 mm \times L_z 10 mm, 90% calcite and dolomite, 8.91% porosity) were inoculated with either mono- or dual-species cultures in the DFR channels. After 24 hours, the cell suspension was removed, and SAB growth continued for 10 days under a 16h/8h day/night photoperiod and 40 $\mu\text{mol m}^{-2} \text{s}^{-1}$ illumination.

3. Methods

SAB-colonized (mono- and dual-species) and control samples (limestone only) were placed in separate desiccator chambers for five days at a constant temperature (T) of 25 °C. Relative humidity (RH) was maintained at 30% (dry condition) or 75% (moist condition) and monitored with digital thermo-hygrometers (Tzone Digital Technology Co., Ltd.). After exposure, samples were analyzed for biofilm coverage (section 3.1), color (section 3.2), and water absorption and wettability (sections 3.3 and 3.4) and compared to pre-exposure conditions.

SAB-colonized and control samples were left for almost two years (from 2023 to 2025) under 30% RH, resulting in dead SABs. Microscopy (section 3.5) was used to assess the presence of living cells and residual organic materials. Water absorption and dispersion tests were also repeated on dead SAB samples and the corresponding control samples. All the experiments were conducted in triplicate.

3.1 Digital Microscope. The percentage of limestone surface covered by live SABs (mono- and dual-species) was assessed using a DinoLite AM7013MZT microscope (Fig. 1b1). Five images per sample were captured and analyzed using ImageJ software [15] to quantify biofilm coverage before and after RH exposure.

3.2 Colorimetric Analysis. Color changes in live and dead SABs and control samples were measured using a Chroma Meter CR400/410 (Konica Minolta - Fig. 1c) in the $L^*a^*b^*$ space calibrated with a white ceramic tile and a black surface provided by the manufacturer. Color change (ΔE) was determined using equation (1) [16]:

$$\Delta E = \sqrt{\Delta L^2 + \Delta a^{*2} + \Delta b^{*2}} \quad (1)$$

where ΔL , Δa^* , and Δb^* represent deviations along the L^* (lightness), a^* (red-green), and b^* (yellow-blue) axes, respectively. Comparisons were made between live SABs before and after treatment and among live and dead SABs and the control samples.

3.3 Contact angle. A 0.03-mL drop of distilled water was deposited on the surface (live and dead SABs and control samples $\theta_{\text{Control}}=57.0^\circ \pm 2.0$) and photographed in frontal geometry using the DinoLite microscope AM7013MZT to record the contact angle θ - Fig. 1b1. Images were processed with ImageJ software, using the function that selects five points: two at the drop's contact angles and three within the drop. Using the *manual point procedure*, the contact angle ($180-\theta$) was then calculated [17].

3.4 Spilling drop test with the infrared thermography. To assess the surface water dynamics on live and dead SABs and control samples, in terms of measuring the evolution over time of the drop's area, the method by Melada et al. was applied in different locations on each sample [11, 18]. A 0.03-mL drop of distilled water was placed on the surface and recorded for 30 seconds at 15 frames/second using AVIO

R550Pro thermal imaging camera (Fig.1d). The thermal files were exported in .csv files, converted to 8-bit grayscale, and analyzed using a bilateral Gaussian filter to reduce noise and segmentation was performed by Yen's method [19].

3.5 Confocal Laser Scanning Microscopy (CLSM). The FilmTracer™ SYPRO™ Ruby Biofilm Matrix Stain (Invitrogen, Italy) was used to visualize the proteinaceous component of the EPS according to the manufacturer's instructions. Fluorescence was excited at 561 nm and detected at 570–620 nm. To detect the autofluorescence of *Synechocystis* cells, an excitation wavelength of 633 nm and emission of 650–750 nm were applied. In addition, the CLSM (Fig. 1b2) was used in reflectance mode with the 488 nm argon line for relief imaging of specimens. Images were captured with a Nikon A1/A1R CLSM and a 20X/NA 0.45 dry lens objective and analyzed with the software Imaris (Bitplane Scientific Software, Switzerland).

4. Results and discussion

The first goal of this study was to investigate how live mono- and dual-species SABs affect surface water absorption and wettability under dry (30% RH) and moist (75% RH) conditions. Dinolite analysis showed no statistically significant changes in SAB surface coverage under any tested conditions for both mono- and dual-species SABs (as reported in Table 1). However, the colorimetric analysis revealed a SAB color change (ΔE) after exposure to different RH. The main shifts occurred in the yellow/blue axes (b^*) and lightness (L^*). The decrease in b^* (Δb^* : -12.7 mono, -4.53 dual at 30% RH; -14.89 mono, -12.02 dual at 75% RH) indicates reduced yellowness in SABs. This, along with an increase L^* (ΔL^* : 7.02 mono, 8.28 dual at 30% RH; 11.14 mono, 9.48 dual at 75% RH), suggests lower concentrations of chlorophyll a, phycocyanin, and carotenoids, as b^* is directly and L^* inversely proportional to these pigments [20]. In all experiments, changes in color parameters were more pronounced in mono than in dual SABs, suggesting that complex microbial communities exhibit greater resilience to environmental variations. The spilling drop test was used to assess water absorption and diffusion on stone surfaces without and with SABs under dry (30%RH) and moist (75%RH) conditions. The drop area percentage increase ($\Delta Area\%$, y-axis) has been assessed using a semi-logarithmic plot with time in the x-axis. Fig.2 reports the results of the 2023 tests, with the SABs mono-species smaller increase (25%, light green and gray lines) than dual-species (55%, dark green and black lines) at both RH (dark lines for dry conditions; green lines wet conditions) within the first 5 seconds.

Overall, these results indicated that, at both RH levels, the stone alone displayed significantly higher wettability and capillary absorption compared to the SAB-colonized samples. Similarly, in SAB-colonized samples, contact angle values increased slightly as RH decreased, suggesting a general hydrophobic behavior of the biofilm, particularly at low RHs (Tab. 1). These findings confirm that SABs alter the stone's surface properties, making it more hydrophobic, in agreement with previous biofilms studies on different types of stone [21, 22]. Increasing evidence suggests that SABs can have neutral or even bioprotective effects by reducing stone's susceptibility to sudden water content variations [23, 24].

The second aim of this study was to explore whether dead mono- and dual-species SABs affect surface properties in terms of water absorption and wettability. The samples were kept at 30% RH for almost two years (from 2023 to 2025) and analyzed

using CLSM to visualize any remaining living cells. The captured images showed no autofluorescence from chlorophyll, confirming the absence of cyanobacterial cells.

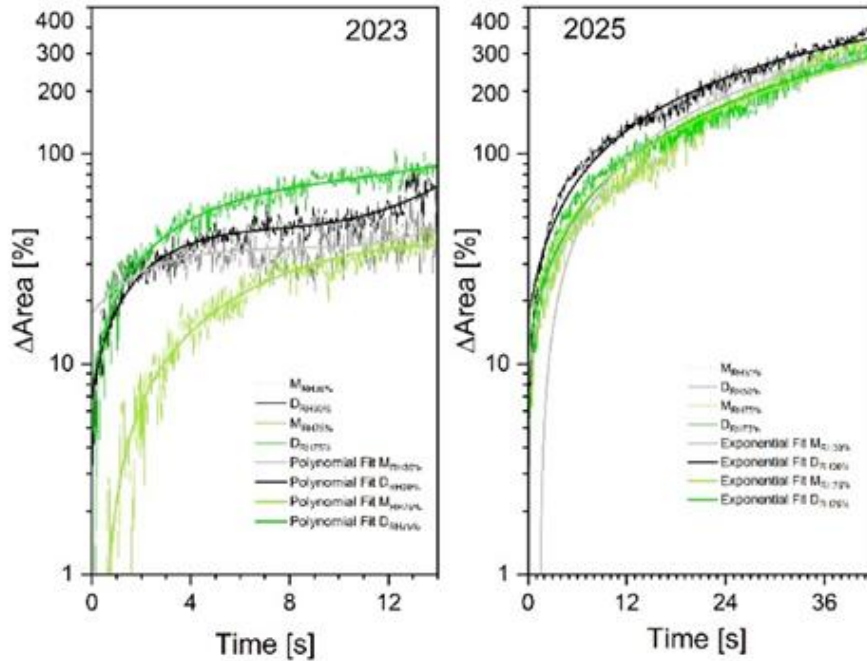


Fig. 2. Temporal evolution of the drop size represented as a percentage increase relative to the instant of drop deposition, with an exponential fit in a semi-logarithmic scale, thick line. 2023 results refer to live SAB samples, 2025 results refer to dead SABs. Green lines result at 75% RH, and dark-grey lines at 30% RH (M=mono and D=dual).

The colorimetric parameter ΔE provided additional information on the residual presence of cells on the surface. The ΔE values revealed a high similarity between the color of dead SAB samples and that of the uncolonized stone. According to Mokrzycki and Tatol [25], ΔE values ranging from 0.5 to 3.0 indicate a slightly perceptible color difference (Tab.1). Despite the absence of cells, dead SAB samples showed a strong fluorescent signal corresponding to proteinaceous material (Fig. 3).

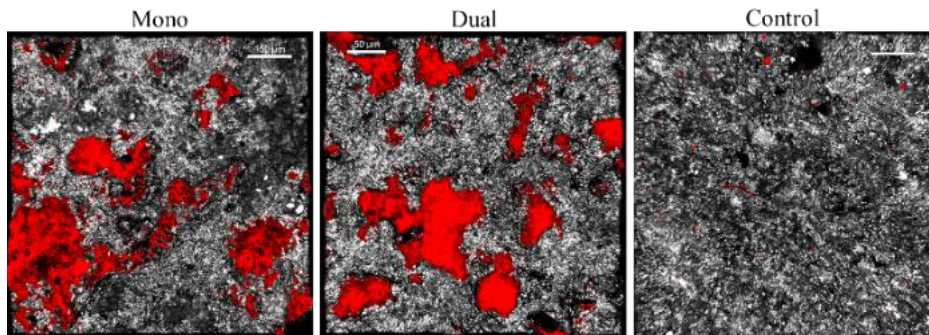


Fig. 3. CLSM images of the dead SABs and corresponding control samples. Color key: proteinaceous material remaining on the stone (red); stone surface (gray). The bars in the CLSM images represent 150 μm .

This material likely originates from the EPS and intracellular biomolecules released after cell lysis. Contact angle results (Tab. 1) showed that even dead SABs had a higher contact angle than the control samples ($\theta_{\text{Control}}=57.0^\circ\pm 2.0$), indicating that residual proteinaceous material reduces stone wettability.

The spilling drop test results show a ΔArea increase when passing from 30%RH to 75% RH. Specifically, within the first 10 seconds, the drop area (Fig. 2, 2025) increases by 70% under moisture conditions (green lines) and about 100% in dry conditions (black and grey lines). The best fit of the drop area increase follows a dynamic growth model (equation 2), similar to those reported in the literature [26, 27]:

$$\ln(\Delta\text{Area}) = A_1 - A_0 * \exp(k * t) \quad (2)$$

where A_1 is the maximal area the drop may reach over time t (i.e., upper asymptote); A_0/A_1 is the growth range, and k is the growth rate. The obtained parameters under the different scenarios of live and dead SABs and RHs are reported in Tab 1.

Table 1. $\Delta\text{Coverage}$ (ΔC) i.e., difference between the final coverage % (after RH exposure) and the starting coverage % (before exposure). ΔE_1 , comparing live samples before and after RH exposure; ΔE_2 , comparing live and dead SABs with non-colonized limestone. CA Contact Angle. RT 63% Response Time to reach 63% of (A_1-A_0).

	Live SABs RH 30%		Live SABs RH 75%		Dead SABs RH 30%		Dead SABs RH 75%	
	Mono	Dual	Mono	Dual	Mono	Dual	Mono	Dual
ΔC (%)	-2.69 \pm 4.2	0.41 \pm 0.75	-1.94 \pm 10.28	5.12 \pm 7.14	-92.55 \pm 5.17	-94.97 \pm 1.73	-81.46 \pm 6.80	-80.22 \pm 5.06
ΔE_1	14.58 \pm 1.58	9.55 \pm 0.97	18.75 \pm 1.12	15.78 \pm 0.48	-	-	-	-
ΔE_2	42.6 \pm 1.8	55.1 \pm 1.4	40.7 \pm 1.3	35.5 \pm 1.5	2.2 \pm 1.6	2.5 \pm 1.8	1.6 \pm 1.4	1.3 \pm 1.1
CA	99.9 $^\circ$ \pm 1.5	112.7 $^\circ$ \pm 4.8	92.3 $^\circ$ \pm 2.0	106.3 $^\circ$ \pm 1.0	86.1 $^\circ$ \pm 3.0	89.0 $^\circ$ \pm 2.0	80.5 $^\circ$ \pm 3.0	88.0 $^\circ$ \pm 2.0
A_1	62.0	79.2	47.3	106.5	848.7	967.6	61520.1	14283.8
A_0	39.5	64.8	51.8	99.0	862.3	952.0	61530.1	14272.3
k	0.05	0.09	0.12	0.14	0.01	0.01	0.0001	0.0005
R^2	0.47	0.81	0.91	0.95	0.95	0.98	0.97	0.97
RT 63%	13.1	10.1	10.0	7.4	102.2	99.3	8529.4	2537.2

As mentioned earlier, live SABs showed a higher water absorption rate compared to the control samples, particularly at RH 75%. In contrast, high RH inhibited water absorption in dead SABs rather than promoting it. Dead mono and dual-species SABs showed no difference in the final water absorption kinetic. However, dead dual-species SABs absorbed water 3.5 times faster than mono-species SABs. In live SABs, the response time to reach the maximal asymptotic water absorption value was independent of RH and species number. In dead dual-species SABs, the response time was shorter than mono species SABs. At RH 75%, live SABs absorb water exponentially faster than dead SABs, with time reductions of up to 850 times for mono-species SABs and 318 times for dual-species SABs. The inhibition of water absorption in dead SABs, particularly under high RH conditions, represents a critical breakthrough in heritage

conservation and restoration. The findings indicated that increasing RH led to a significant reduction in the specific water absorption rate, with this effect being more pronounced in dual-species SABs, ultimately reducing water absorption efficiency by up to six times in high RH conditions providing a protective barrier against moisture penetration.

4. Conclusion

This study investigated the impact of SABs on limestone surface properties under dry (30% RH) and moist (75% RH) conditions, focusing on how live and dead SABs influence surface water sorption and wettability. Overall, the results demonstrated that live SABs increase surface hydrophobicity and reduce water sorption, regardless of environmental conditions. Notably, these new surface properties persist even in dead SABs, likely due to the presence of proteinaceous material from residual EPS and lysed cells. The residual biomaterial affects surface water dynamics while almost preserving the stone's natural color. Unlike traditional conservation strategies that rely on synthetic hydrophobic coatings—often associated with material incompatibility, long-term degradation, and environmental concerns—naturally occurring biomaterials from dead SABs provide a protective barrier against moisture penetration and weathering in limestone. The present research paves the way for a completely natural, eco-friendly solution to mitigate water-induced deterioration, offering a sustainable alternative to synthetic conservation treatments. These findings have critical implications for material conservation, moisture management, and biological coatings, where regulating RH and biofilm viability can either optimize or hinder water absorption processes.

References

1. Sesana, E., Gagnon, A., Ciantelli, C., Cassar, J., Hughes, J. Climate change impacts on cultural heritage: A literature review. *WIREs Climate Change* (2021). doi.12.10.1002/wcc.710
2. Gaylarde, C., Little, B. Biodeterioration of stone and metal - Fundamental microbial cycling processes with spatial and temporal scale differences, *Science of The Total Environment*, 823, 153193 (2022). doi.10.1016/j.scitotenv.2022.153193
3. Gorbushina, A. Life on the rocks. *Environmental Microbiology*, 9(7), 1462-2912 (2007) doi.10.1111/j.1462-2920.2007.01301.x
4. Villa, F., Stewart, P. S., Klapper, I., Jacob, J. M., Cappitelli, F., Subaerial Biofilms on Outdoor Stone Monuments: Changing the Perspective Toward an Ecological Framework. *BioScience*, 285–294, 66(4) (2016). doi.10.1093/biosci/biw006
5. Gadd, G. M., Dyer, T.D. Bioprotection of the built environment and cultural heritage. *Microbial Biotechnology*, 10(5), 1152-1156 (2007). doi.org/10.1111/1751-7915.12750
6. Villa, F., Cappitelli, F. The Ecology of Subaerial Biofilms in Dry and Inhospitable Terrestrial Environments. *Microorganisms*, 7(10), 380 (2019). doi.10.3390/microorganisms7100380
7. Gadd, G.M. Geomicrobiology of the built environment. *Nature Microbiology*, 16275, 2(4) (2017). doi.10.1038/nmicrobiol.2016.275
8. Negi, A., Sarethy, I.P. Microbial Biodeterioration of Cultural Heritage: Events, Colonization, and Analyses. *Microb Ecol* 78, 1014–1029 (2019). doi.10.1007/s00248-019-01366-y
9. Liu, X., Koestler, R.J., Warscheid, T. *et al.* Microbial deterioration and sustainable conservation of stone monuments and buildings. *Nat Sustain* 3, 991–1004 (2020). doi.10.1038/s41893-020-00602-5

10. Vázquez, N. D., Silva, B., Prieto, B. Influence of the properties of granitic rocks on their bioreceptivity to subaerial phototrophic biofilms, *Science of The Total Environment*, 610-611, 44-54 (2018). doi.10.1016/j.scitotenv.2017.08.015
11. Melada, J.; Villa, F.; Giudici, M.; Battaglia, I.; Carangelo, E.; Marzanni, A.; Ripamonti, D.; Ludwig, N. Investigating the Role of Subaerial Biofilms in Cultural Heritage Conservation with Infrared Thermography. *Eng.Proc.*, 51, 18 (2023). doi.10.3390/engproc2023051018
12. Yong-Hui L., Ji-Dong G. A more accurate definition of water characteristics in stone materials for an improved understanding and effective protection of cultural heritage from biodeterioration. *International Biodeterioration & Biodegradation*, 166 (2022), doi.org/10.1016/j.ibiod.2021.105338
13. Alfano F.R.A., Palella B.I. , Riccio G., Moisture in historical buildings from causes to the application of specific diagnostic methodologies. *Journal of Cultural Heritage*, 61, 150-159 (2023). doi.10.1016/j.culher.2023.04.001
14. Villa, F., Pitts, B., Lauchnor, E., Cappitelli, F., & Stewart, P. S. Development of a laboratory model of a phototroph-heterotroph mixed-species biofilm at the stone/air interface. *Frontiers in Microbiology*, 6(NOV) (2015). doi.10.3389/fmicb.2015.01251
15. Rasband, W. S. ImageJ, US national institutes of health (2007). [rsb.info.nih.gov/ij/\(1997-2007\)](http://rsb.info.nih.gov/ij/(1997-2007))
16. EN 15886:2010. Conservation of Cultural Property-Test Methods Colour Measurements of Surfaces. CEN: Brussels, Belgium (2010).
17. Buahom P. Measuring the Contact Angle using ImageJ with Contact Angle plug-in (2018)
18. Melada J., Arosio P., Gargano M. and Ludwig N.; Multi-instrumental characterization of porous media: the role of spilling drop test. Measurement. In *Proceedings of 15th Quantitative InfraRed Thermography Conference. QIRT journal* 1-6 (2020). doi.10.21611/qirt.2020.061
19. Sezgin, M., & Sankur, B. Survey over Image Thresholding Techniques and Quantitative Performance Evaluation. *J. Electron Imaging*, 146–165 (2004).
20. Sanmartín, P., Aira, N., Devesa-Rey, R., Silva, B., & Prieto, B. Relationship between color and pigment production in two stone biofilm-forming cyanobacteria. *Biofouling*, 26(5), 499–509 (2010). doi.10.1080/08927011003774221
21. Schröer, L., De Kock, T., Godts, S., Boon, N., Cnudde, V. The effects of cyanobacterial biofilms on water transport and retention of natural building stones. *Earth Surface Processes and Landforms* (2022). doi.10.1002/esp.5355
22. Villa, F., Ludwig, N., Mazzini, S., Scaglioni, L., Fuchs, A. L., Tripet, B., Copié, V., Stewart, P. S., & Cappitelli, F. A desiccated dual-species subaerial biofilm reprograms its metabolism and affects water dynamics in limestone. *Science of the Total Environment*, 868 (2023). doi.10.1016/j.scitotenv.2023.161666
23. Sanmartín, P., Villa, F., Cappitelli, F., Balboa, S., Carballeira, R. Characterization of a biofilm and the pattern outlined by its growth on a granite-built cloister in the Monastery of San Martiño Pinario (Santiago de Compostela, NW Spain). *International Biodeterioration & Biodegradation*, 147 (2020), doi.10.1016/j.ibiod.2019.104871
24. Pinna, D., Mazzotti, V., Gualtieri, S., Voyron, S., Andreotti, A., Favero-Longo, S. E. Damaging and protective interactions of lichens and biofilms on ceramic dolia and sculptures of the International Museum of Ceramics, Faenza, Italy, *Science of The Total Environment*, 877 (2023), doi.10.1016/j.scitotenv.2023.162607
25. W. Mokrzycki and M. Tatol. Color difference Delta E - A survey. *Machine Graphics and Vision*. 20. 383-411 (2011).
26. Bravo, P., Lung, N. S., MacGillivray, K.A., Hammer, B.K., Yunker P.J. Vertical growth dynamics of biofilms, *Proc. Natl. Acad. Sci. U.S.A.*, 120(11) (2023). doi.10.1073/pnas.2214211120
27. Baranyi, J., McClure, P., Sutherland, J., Roberts, T. Modeling bacterial growth responses. *Journal of Industrial Microbiology*. 12. 190-194 (1993). doi.10.1007/BF01584189.